

THEORY OF ULTRASOUND DOPPLER-SPECTRA VELOCIMETRY FOR ARBITRARY BEAM AND FLOW CONFIGURATIONS *

Dan Censor ** and Vernon L. Newhouse

Department of Electrical and Computer Engineering, and Biomedical Engineering
and Science Institute, Drexel University, Philadelphia, PA 19104

ABSTRACT

Conventional ultrasound Doppler velocimetry is based on the frequency shifts produced when the beam axis and the flow direction produce acute angles. Recently it was shown, theoretically as well as experimentally, that by using a pulsed Doppler system with the beam transversely oriented with respect to the flow, the flow velocity can be derived from the limits of the relevant Doppler spectrum. The theory discussed previously was limited to transverse motion, constant flow velocity and uniformly insonified apertures, as well as monochromatic excitation. Presently these results are generalized to take into account arbitrary directions of incidence, effects of velocity gradients, arbitrary apertures and arbitrary source pulses. For uniform apertures and transverse flow, it has been previously shown that the Doppler output spectrum is symmetrical about zero frequency, with its width depending in a straightforward manner on the Doppler effect due to the velocity and the geometry of the problem. For a beam direction oblique to the particle's direction, this spectrum is shifted, so that instead of zero frequency, the reference is the classical Doppler frequency corresponding to the velocity component parallel to the beam. Previously only a constant velocity flow field was considered. It is shown here that for velocity gradients and transverse flows the spectrum remains symmetrical, with the edges corresponding to the maximal velocity, however, the profile becomes peaked at the center. For oblique incidence an asymmetrical spectrum is obtained and its edges are related to the maximal and minimal velocities within the measurement volume.

For the simple case of a long strip transducer discussed previously, it was shown that the Doppler system output spectrum is essentially obtained by convolving the transmitter and receiver aperture functions. The general discussion given here, even for the single particle, is more complicated. Nevertheless, using the reciprocity theorem it is shown that the output spectrum is obtained by convolving the particle excitation spectrum due to monochromatic excitation, with the receiver input spectrum due to a moving monochromatic source, all this shifted to the classical Doppler frequency mentioned above. It is shown that when the excitation, rather than being monochromatic, possesses an arbitrary (narrow band) spectrum, this spectrum, replicated in a prescribed manner, has to be convolved with the spectra derived above.

The spectrum produced by an ensemble of particles is more complicated. The strategy used here is to derive semi-quantitative graphical interpretations for various configurations, and to further substantiate the results by analytically treating simplified models.

* Supported by NSF Grant No. ECS-8219736

** Visiting Professor, on leave of absence from the Department of Electrical and Computer Engineering, Ben Gurion University of the Negev, Beer Sheva, Israel. Supported by the Louis and Bessie Stein Family Foundation Fellowship Program.

INTRODUCTION

Ultrasound Doppler techniques are currently used for analysing motional effects, e.g., in clinical diagnostics of the cardio-vascular system. The common base for such techniques is the phenomenon of frequency shift caused by the motion of scatterers relative to the ultrasound beam axis. Thus for an object moving with velocity $v = v \hat{v}$ at an angle θ with respect to the propagation vector $k = k \hat{k}$ of a plane wave, where \hat{v} , \hat{k} are unit vectors, and $k = \omega_0/c$, ω_0 being the (angular) frequency and c the sound velocity, we get, to the first order in v/c a scattered wave with a frequency shift ¹

$$\omega_d = (2\omega_0 v/c) \cos\theta, \quad \cos\theta = \hat{k} \cdot \hat{v} \quad (1)$$

Only the first order effects in v/c are significant. Higher order effects are negligible for low velocities, and in any case it must be remembered that the whole subject of linear acoustics is based on approximations of the first order in the Mach number. The formula (1) has been derived on the basis of a time harmonic (monochromatic) signal, but is nevertheless used for pulsed Doppler systems, provided the length of individual pulses is much larger than the wavelength of the carrier wave. The effect (1) vanishes for motion perpendicular to the beam axis. However, since all real beams have a finite cross section, i.e., are *not* a plane wave of finite extent, or equivalently, since transducer apertures are finite, Doppler spectra are produced even in the transverse mode. The relation of Doppler spectra to beam geometry has been discussed recently ^{2,3}, on the basis of ray geometrical considerations. Recently it has been shown experimentally ^{4,5} and verified theoretically ⁶ that for beam axis and flow at right angles the amplitude Doppler spectrum produced by a uniformly insonified aperture of a long strip transducer possesses a triangular profile, and that the edge frequencies of the spectrum profile, which are relatively easy to measure, are related to the velocity by means of a simple formula.

In order to better understand the Doppler spectra discussed below, a short review of the principles and properties of typical Doppler ultrasound systems is appropriate ⁷. Continuous Doppler systems emit a frequency ω_0 and receive Doppler shifted spectral components of various frequencies ω . In the simplest case $\omega_d = \omega_0 - \omega$ is given by (1). The received signal is multiplied by the carrier frequency ω_0 and low-pass filtered, thus yielding ω_d . In pulsed Doppler systems periodic pulses of center frequency ω_0 and a repetition (angular) frequency Ω are transmitted. At the receiver, after downshifting the signal by ω_0 , it is sampled at the pulse repetition frequency Ω with a gate pulse whose time delay relative to the transmitted signal determines the distance of the so called range cell or measurement volume. It has been shown ⁸ that, if the beam is almost parallel to the flow and the range cell is short enough, the Doppler system output amplitude spectrum

$S_0(\nu)$ is a frequency scaled replica of the echo amplitude spectrum $S(\nu)$, given by

$$S_0(\nu) = \frac{1}{|\gamma|} S(\nu/\gamma), \quad \gamma = \omega_d/\omega_0 \quad (2)$$

This then is the effect of the pulsed Doppler system instrumentation when the effect of the transmitter and receiver's finite aperture can be neglected.

Previously, transverse motion and constant velocity have been assumed. Furthermore, in the past only monochromatic (CW) signals were considered, which is adequate for very long pulses (i.e., pulses containing many cycles of the carrier wave). The model used for the present analysis is more realistic and general, addressing the questions of arbitrary flow angles, various transducer aperture geometries and arbitrary transmitter pulse shapes. The cases treated earlier⁶ are special cases. It is assumed in the present study, as was done previously, that the particles producing the Doppler effects are small, that their positions are uncorrelated, and that their motion coincides with the ambient fluid's velocity field.

While studying the transverse flow case⁶, it became clear that there are two main considerations underlying the theory for Doppler spectra. The first is the well known reciprocity principle⁹, which states that the spatial properties (i.e., the radiation pattern) of a transducer are the same whether it acts as a transmitter or a receiver. Secondly, for the special case of constant velocity and long strip transducer, it was shown that the Doppler amplitude spectrum has a shape which is obtained by convolving the transmitter and receiver aperture functions. A more general formulation is given below, again involving convolution of two spectra which are determined by the transverse velocity component and the transmitter and receiver's radiation patterns.

The remainder of the paper is arranged as follows. Exploiting the results obtained from the reciprocity and spectra convolution principles, and assuming monochromatic signals, Doppler spectra produced by transverse and oblique flows are analysed for various transducer apertures and flow configurations. Where the analysis becomes too cumbersome we revert to semi-quantitative graphical constructions. In Appendices B-D analytical discussions are given which serve to illustrate and substantiate the graphical results. In order to facilitate analysis, the examples chosen are highly idealized. For arbitrary narrow band pulses, as found in pulsed Doppler systems, it is shown that the single frequency excitation spectrum has to be convolved with the scaled longitudinal Doppler spectrum given in (2).

GENERAL THEORY AND THE DOPPLER SPECTRUM CONVOLUTION THEOREM

The Particle Excitation Field

It is well known that at large distances from the source, the solution of the wave equation can be approximated by a spherically outgoing wave, multiplied by the so called scattering amplitude¹⁰, or directivity function. Thus we have

$$\psi = \psi_0 \frac{1}{r} e^{ikr - i\omega t} g(\hat{r}), \quad k = \omega/c \quad (3)$$

where r is the distance from the origin, ω is the (angular) frequency, c is the sound speed and $\hat{r} = \hat{r}(\theta, \phi)$ is a unit vector depending on directions θ , the polar angle, and ϕ the azimuthal angle. See Fig.1. The quantity ψ can be any solution of the acoustical wave equation, e.g., the velocity potential. The

constant ψ_0 , which also takes care of units involved, is arbitrary and can be set equal to unity. We can also represent ψ in terms of the source amplitude or aperture function $\psi_a(\rho)$, dependent on the radius vector ρ ,

$$\psi = e^{-i\omega t} \int \frac{1}{R} e^{ikR} \psi_a(\rho) dv(\rho), \quad R = |\mathbf{r} - \rho| \quad (4)$$

and for cases where the source is distributed on a surface, (4) becomes a surface integral with $ds(\rho)$ replacing $dv(\rho)$. Furthermore, it is now assumed that this surface is planar and perpendicular to the ray $\theta = 0$, as in Fig. 1. In the far field

$$R \approx \mathbf{r} \cdot \hat{\rho} = r - \rho \cdot \hat{r} / r = r - \xi x / r - \eta y / r \quad (5)$$

leading to the Fraunhofer diffraction approximation¹¹ of (4)

$$\begin{aligned} \psi &\approx \frac{1}{r} e^{ikr - i\omega t} \int e^{-ikr \cdot \rho} \psi_a(\rho) ds(\rho) \\ &\approx \frac{1}{r} e^{ikr - i\omega t} \int e^{-ik \xi x / r - ik \eta y / r} \psi_a(\xi, \eta) ds(\xi, \eta) \end{aligned} \quad (6)$$

Comparison of (3), (6) shows¹² that ψ_a, g constitute a two dimensional Fourier transform pair.

Consider now a single particle moving according to

$$\mathbf{r} = \mathbf{r}_0 + \mathbf{v}t$$

$$|\mathbf{r}| = r = \left[(\mathbf{r}_0 + \mathbf{v}t) \cdot (\mathbf{r}_0 + \mathbf{v}t) \right]^{1/2} = r_0 + \mathbf{v} \cdot \mathbf{r}_0 t$$

$$\hat{\mathbf{r}} = \mathbf{r} / r = \hat{\mathbf{r}}_0 + \mathbf{v}t / r_0 \hat{\mathbf{r}}_0 (\hat{\mathbf{r}}_0 \cdot \mathbf{v}) t / r_0 = \hat{\mathbf{r}}_0 + \mathbf{v}_+ t / r_0 \quad (7)$$

where \mathbf{r}_0, \mathbf{v} are constants and the time origin is immaterial, as explained below, and \mathbf{v}_+ is the component of the velocity perpendicular to \mathbf{r}_0 . This analysis is valid for short time intervals only, such that the leading terms retained in (7) provide an adequate approximation. This is applicable to focused transducers, where $r_0 = F_0$ becomes the focal length and $\mathbf{v}_+ t / r_0 \ll 1$ because the directivity function is very sharp, hence the distance $\mathbf{v}_+ t$ the particle traverses in the insonified focal region is small compared to F_0 . Substituting (7) in (3) yields $g(\hat{\mathbf{r}}[t])$, and substitution of (7) in (6) yields

$$g(\hat{\mathbf{r}}[t]) = \int e^{-ik\hat{\mathbf{r}}_0 \cdot \rho} \psi_a(\rho) ds(\rho) \quad (8)$$

where it is noticed that $e^{-ik\hat{\mathbf{r}}_0 \cdot \rho} = 1$ because $\hat{\mathbf{r}}_0 \cdot \rho = 0$. Thus (8) yields $g(\hat{\mathbf{r}}[t])$ as a function of t and provides a relation between the field exciting the particle and the aperture function $\psi_a(\rho)$. Corresponding to (8) we define a spectrum

$$G_\omega(\nu) = F g(\hat{\mathbf{r}}[t]) \quad (9)$$

where F denotes the Fourier transform and ω indicates the excitation frequency in (8). For the special case of the long strip transducer it is shown below that $G_\omega(\nu)$ replicates the aperture function.

The Doppler Spectrum Convolution Theorem

Essentially, this theorem follows from the well known reciprocity principle⁹ for the interchange of source and observer, mentioned above. For simplicity let us first assume $\mathbf{v} \cdot \mathbf{r} = 0$, i.e., transverse motion. For this case $r = r_0$ as in (3). The spectrum exciting a particle is given by

$$\delta(\nu - \omega) * G_\omega(\nu) \quad (10)$$

where $\delta(\nu - \omega)$ is due to the factor $e^{-i\omega t}$ in (3). The field exciting the particle is therefore

$$\psi_e = \frac{1}{r_0} e^{ikr_0 - i\omega t} \int e^{-i\nu t} G_\omega(\nu) d\nu \quad (11)$$

In response to a unit amplitude excitation at frequency $\nu = \omega + \nu$, the particle radiates a field

$$\sigma(\nu) \frac{1}{r} e^{ik' r' - i\nu' t}, \quad k' = \nu' / c \quad (12)$$

where r' is the distance from the particle. The small particle scattering amplitude $\sigma(\nu')$ is constant with respect to directions, but depends on the excitation frequency (e.g., according to the Rayleigh scattering theory^{10,11}). According to the reciprocity principle⁹, if the particle acts as a source at frequency ν' , it will produce in the transducer, now acting as receiver, a field depending on the location of the source within the transducer's radiation pattern $g_\nu(\hat{r})$. Since obviously $r' = r = r_0$, at the receiver we obtain the signal

$$\psi_s = \sigma(\nu') \frac{1}{r_0} e^{-i\nu' t'} g_\nu(\hat{r}), \quad t' = t - r_0/c \quad (13)$$

where t' is the retarded time referred to the particle's position. Thus in (13) we have

$$g_\nu(r[t']) = \int e^{-i\mu t'} G_\nu(\mu) d\mu \quad (14)$$

where for $\nu' = \omega$, $g_\nu(\hat{r})$ and $g_\omega(\hat{r})$ become identical. Combining (11)-(14) the received field is given by

$$\begin{aligned} \psi_R &= \frac{1}{r_0^2} e^{ikr_0} \int [d\nu G_\omega(\nu) \sigma(\nu') e^{-i\nu' t'} \int e^{-i\mu t'} G_\nu(\mu) d\mu] \\ &= \frac{1}{r_0^2} e^{ikr_0 - i\omega t'} \int [d\nu G_\omega(\nu) \sigma(\nu') e^{-i\nu t'} \int d\mu e^{-i\mu t'} G_\nu(\mu)] \quad (15) \end{aligned}$$

As (15) stands, the two integrations are not separable, since ν of the first integral appears in G_ν of the second one. However, since the creation of the spectrum is already a first order velocity effect, we are justified in neglecting higher order effects appearing in (15). In other words, the approximation is justified because $\sigma(\nu')$, G_ν are narrow band functions with respect to ν' . Thus we write

$$\begin{aligned} \sigma(\nu') &= \sigma(\omega) + \frac{\partial \sigma}{\partial \omega} \nu + \dots \approx \sigma(\omega) \\ G_\nu(\nu) &= G_\omega(\mu) + \frac{\partial G_\omega}{\partial \omega} \nu + \dots \approx G_\omega(\mu) \quad (16) \end{aligned}$$

Since ω is a constant for monochromatic excitation $\sigma(\omega)$ is taken to be a constant, and $G_\nu \approx G_\omega$. Consequently (15) becomes

$$\psi_R = K e^{-i\omega t'} \left[\int d\nu e^{-i\nu t'} G_\omega(\nu) \right]^2 \quad (17)$$

where K absorbs the extra terms in (15). Inasmuch as (17) describes a product of time domain functions, the amplitude spectrum of the received signal is given by

$$S(\nu) = \delta(\nu - \omega) * G_\omega(\nu) * G_\omega(\nu) \quad (18)$$

The Doppler spectrum convolution theorem (18) states that the spectrum $S(\nu)$ measured at the receiver is obtained by convolving the excitation spectrum of the moving particle by itself, then shifting the zero reference to the transmitter frequency ω . As explained above, in an ultrasound Doppler system the frequency is downshifted by ω , yielding $S_0(\nu)$, i.e.,

$$S_0(\nu) = G_\omega(\nu) * G_\omega(\nu) \quad (19)$$

Thus far, in calculating the effect of the particle velocity on its excitation, only the velocity effect on $g(\hat{r}[t'])$ was considered. But when $v \cdot \hat{r} \neq 0$, then the spherical wave part of (3), (6) is affected too. According to (7) we obtain

$$\begin{aligned} e^{ik(r_0 + v \cdot \hat{r}_0) - i\omega t} / (r_0 + v \cdot \hat{r}_0 t) &\approx e^{ikr_0 - i\omega_1 t} / r_0 \\ \omega_1 &= \omega(1 - v \cdot \hat{r}_0) / c \quad (20) \end{aligned}$$

where in the denominator the velocity effect is neglected, due to the fact that the observation time t is restricted, i.e., when the flow moves the particle outside the focal region, it is eventually lost, as far as the performance of the system is concerned. However, in the exponent a Doppler frequency shift is obtained. This means that instead of (10) we now have

$$\delta(\nu - \omega_1) * G_{\omega_1}(\nu) \approx \delta(\nu - \omega_1) * G_\omega(\nu) \quad (21)$$

where ω_1 is defined in (20), and the same argument leading to the approximation (16) is applied in (21). Similarly (18), the echo amplitude spectrum, is now modified

$$\begin{aligned} S(\nu) &= \delta(\nu - \omega_2) * G_\omega(\nu) * G_\omega(\nu) \\ \omega_2 &= \omega(1 - 2v \cdot \hat{r}_0 / c) \quad (22) \end{aligned}$$

and in the geometry of Fig. 1 $v \cdot \hat{r}_0 = v \cdot \hat{z}$.

Instead of monochromatic excitation, consider now a transmitter pulse whose spectrum $H(\omega)$ is given. In this case the contributions of all spectral components must be properly added. Consider first the case of transverse motion. Instead of ψ_R , (15), we have the integral

$$\int d\omega H(\omega) \psi_R \quad (23)$$

Inasmuch as ψ_R (15) or its approximate form (17) involve integration, (23) becomes a non-separable integral. Only for narrow-band pulses, such that most energy is concentrated in the vicinity of the carrier frequency ω_0 , will the general expression (23) become separable. Again we have a narrow band approximation as in (16)

$$G_\omega(\nu) = G_{\omega_0}(\nu) + \frac{\partial G_\omega}{\partial \omega} \Big|_{\omega = \omega_0} (\omega - \omega_0) + \dots \approx G_{\omega_0}(\nu) \quad (24)$$

and similarly for the functions $G_\nu, \sigma(\nu')$ in (15), and instead of (17) we now have

$$\psi_R = K \left[\int e^{-i\omega t'} H(\omega) d\omega \right] \left[\int d\nu e^{-i\nu t'} G_{\omega_0}(\nu) \right]^2 \quad (25)$$

constituting independent integrals. Corresponding to (18), the spectrum is given by

$$S(\nu) = H(\nu) * G_{\omega_0}(\nu) * G_{\omega_0}(\nu) = H(\nu) * S_0(\nu) \quad (26)$$

$S_0(\nu)$ given by (19). This is a very convenient result because, as shown below, we are able to extract information about the velocity from $G_{\omega_0}(\nu) * G_{\omega_0}(\nu)$. If narrow-band pulses are used such that (26) is valid, then by deconvolving $H(\nu)$ out of (26) we can restore (19). In most practical cases the pulse spectrum is almost monochromatic, hence the deconvolution is not necessary. The same considerations apply to oblique motion, with the appropriate modifications discussed below.

For oblique incidence and monochromatic excitation (22) applies. When the transmitter emits a signal having a spectrum $H(\nu)$, corresponding to a time domain signal $h(t) = \int H(\nu) e^{-i\nu t} d\nu$, then the particle is excited by frequencies $\nu_1 = \nu \alpha = \nu(1 - v \cdot \hat{r}_0 / c)$, i.e., by a signal $h_1(t) = \int H(\nu) e^{-i\nu_1 t} d\nu = \int H_1(\nu_1) e^{-i\nu_1 t} d\nu_1$, where by change of variable

$$H_1(\nu_1) = \frac{1}{\alpha} H\left(\frac{\nu_1}{\alpha}\right) \quad (27)$$

Consequently, except for the amplitude factor $\frac{1}{\alpha}$, the spec-

trum $H(\frac{\nu}{\alpha})$ appears as a compressed or expanded replica of the original $H(\nu)$. The echo signal involves $\nu_2 = \nu\beta = \nu(1-2v \cdot \hat{r}_0/c)$ and the spectrum at the receiver will be given by

$$S(\nu) = \frac{1}{\beta} H(\frac{\nu}{\beta}) * G_{\omega_0}(\nu) * G_{\omega}(\nu) \quad (28)$$

where $\frac{1}{\beta} H(\frac{\nu}{\beta})$ is the spectrum of the time domain function $h_2(t)$ picked up by the receiving transducer. For $\beta = 1$, i.e., transverse flow, (26) is obtained as a limiting case. The signal processing performed on the pulse Doppler system has been analysed before⁸, and it has been shown that the detected signals may appear time inverted, depending whether $\beta > 1$ or $\beta < 1$. The corresponding spectrum is given in (2). Consequently the output spectrum corresponding to (19) is now modified, yielding

$$S_0(\nu) = \frac{1}{\gamma} H(\nu/\gamma) * G_{\omega_0}(\nu) * G_{\omega}(\nu), \quad \gamma = |1-\beta| \quad (29)$$

Note that in (29) $H(\nu/\gamma)$ depends on the longitudinal velocity component $v \cdot \hat{r}_0$ while $G_{\omega_0}(\nu)$ depends on v_+ , the transverse component. A simple proof of (29) is given in Appendix A.

Up to now the spectrum produced by a single particle has been discussed. We assume that the particles have random uncorrelated positions, but their velocity is deterministic, coinciding with the ambient flow velocity field. Hence all particles possessing the same velocity \mathbf{v} produce, according to (19), (29) the same spectrum. The total effect of this incoherent process is obtained by adding intensities (rather than amplitudes, as in the case of coherent fields). Let us denote the amplitude (i.e., square root of the intensity) spectrum due to all particles having the same velocity \mathbf{v} by $S(\nu, \mathbf{v})$. The total amplitude spectrum, taking into account all velocity components appearing in the measurement volume is therefore given by

$$S(\nu) = \left\{ \int d\mathbf{v} [S(\nu, \mathbf{v})]^2 f(\mathbf{v}) \right\}^{1/2} \quad (30)$$

Note that the spatial distribution of the velocity field does not appear in (30), i.e., the system cannot resolve positions within the range cell.

This is the general theory for Doppler spectra. Special cases of interest will be discussed below.

TRANSVERSE MOTION, CONSTANT VELOCITY

The long strip transducer: This case has been analysed previously⁸. It is included here to serve as a simple example for the use of the theory and to provide continuity. Let $r_0 = F_0$ be the focal length, and \mathbf{v} in the \mathbf{x} direction perpendicular to the beam axis and the direction \mathbf{y} along the strip. According to (8), (9) we obtain for (10)

$$\delta(\nu-\omega) * G_{\omega}(\nu) = \delta(\nu-\omega) * \psi_a(kv\xi/F) = \psi_a(\omega[1 + \frac{v}{c} \frac{\xi}{F}]) \quad (31)$$

For a uniformly insonified aperture ψ is constant in the range $-W/2 \leq \xi \leq W/2$ and zero for $|\xi| > W/2$, hence ψ_a and $S(\nu)$, (18), are as shown in Fig. 2(a), 2(b), respectively. Clearly the edges of the spectrum correspond to the Doppler effect produced by the edges of the transducer, and these extreme frequencies are quite easy to measure. If W, F_0 are known, the velocity is easily derived. For this case of constant velocity the computation of $S(\nu)$ as in (30) is automatically taken into account, hence (31) applies to a single particle, as well as to a

stream of uncorrelated particles distributed at arbitrary locations \mathbf{y} along the strip.

The circular aperture transducer: Another case of interest is derived from (6) when the aperture has angular symmetry, i.e., $\psi_a = \psi_a(\rho)$. The scatterer trajectory is now written as

$$\mathbf{r} = \hat{\mathbf{y}}a + \hat{\mathbf{z}}vt \quad (32)$$

where a is the distance of the particle from the beam axis at time $t = 0$. Consequently (3), (6) now prescribe

$$\begin{aligned} g(\hat{\mathbf{y}}a + \hat{\mathbf{z}}vt) &= \int_0^{2\pi} d\beta \int_0^{b_0} \rho d\rho e^{-ik\rho \cos(\beta-\phi) \sin\theta} \psi_a(\rho) \\ &= 2\pi \int_0^{b_0} \rho d\rho \psi_a(\rho) J_0(k\rho \sin\theta) \end{aligned} \quad (33)$$

(which is usually referred to as the Hankel transform). Here ϕ can be chosen $\phi = 0$ i.e., the origin of ϕ is immaterial because of the angular symmetry, and

$$\sin\theta = \left[\frac{a^2 + (vt)^2}{r^2} \right]^{1/2} \quad (34)$$

For the uniformly insonified circular aperture (6) yields¹²

$$\psi = 2\pi b_0^2 \frac{e^{ikr_0 - i\omega t}}{r_0} \frac{J_1(b_0 k \sin\theta)}{b_0 k \sin\theta} \quad (35)$$

where $\phi = 0$ is assumed and b_0, J_1 denote the aperture radius and the nonsingular Bessel function of order one, respectively. For $\theta \approx \sin\theta$ in (17) r_0 can be replaced by the focal length F_0 and this is substituted in (35). The spectrum exciting a single particle is therefore given by

$$\delta(\nu-\omega) * G(\nu, \mathbf{y}) = \delta(\nu-\omega) * F \left\{ \frac{J_1(b_0 k [v^2 t^2 + y^2]^{1/2} / F_0)}{b_0 k [v^2 t^2 + y^2]^{1/2} / F_0} \right\} \quad (36)$$

From (18) it follows that the received echo due to particles with a given offset \mathbf{y} is proportional to

$$S(\nu, \mathbf{y}) = \delta(\nu-\omega) * G_{\omega}(\nu, \mathbf{y}) * G_{\omega}(\nu, \mathbf{y}) \quad (37)$$

and if the density with respect to \mathbf{y} is constant, then according to (29) we obtain

$$S(\nu) = \left\{ \int d\mathbf{y} [S(\nu, \mathbf{y})]^2 \right\}^{1/2} \quad (38)$$

The transformation in (36) and the integration (38) are too complicated for analytic computation. We therefore proceed by first presenting a semi-quantitative argument, aided by graphical construction, then in Appendix B the conclusions are supported by analysis of a special idealized model.

It is clear from (36) that the spectrum exciting a single particle depends on \mathbf{y} . For $y \gg vt$ the spectrum becomes proportional to $\delta(\nu-\omega)$, i.e., all Doppler spectra effects disappear. For $\mathbf{y} = 0$, i.e., for a particle going through the beam's axis, the time modulation is more pronounced, hence the spectrum is broader. We do not attempt to compute these spectra, however, for different \mathbf{y} such that $y_1 < y_2 < y_3$ we expect from (37) increasingly broader spectra, as sketched in Fig. 3. It is therefore plausible to assume that (38) will yield a peaked amplitude spectrum, as opposed to the triangular shape in Fig. 2. The results are also supported by simulations given by Bascom et al.³, although they consider a CW Doppler system. According to the above explanation, the ends of the spectrum are due to particles going through the beam axis $\mathbf{y} = 0$, and therefore undergoing the strongest modulation. In (38) this

corresponds to $G(\nu, 0) = F \left\{ \frac{J_1(b_0 k v t / F_0)}{b_0 k v t / F_0} \right\}$. It is easy to show that these extreme frequencies correspond to Doppler effects produced by the transducer's rim. Consider (8) for maximum $v \cdot \rho = v \rho$, i.e., (8) describes Doppler shifted waves and the maximum shift Δf_{\max} , at the rim $\rho = b_0$ is given by

$$\Delta f_{\max} = \omega \frac{v b_0}{c F_0} \quad (39)$$

exactly as in the case of the long strip transducer. After convolving the signals as in (37), the edges of the spectrum in Fig. 3 will be at frequencies

$$\nu_{\max} = \omega \left(1 + \frac{v b_0}{c F_0} \right), \quad \nu_{\min} = \omega \left(1 - \frac{v b_0}{c F_0} \right) \quad (40)$$

Some of the features derived above can be obtained from the analysis of a circular aperture with Gaussian apodization, see Appendix B.

OBLIQUE MOTION, CONSTANT VELOCITY

The long strip transducer: Once again we consider the long transducer, oriented in the y direction. The particles possess now a velocity component in the radial direction, i.e., in the z direction for focused beams (Fig. 1). From (7) it is clear that this velocity component cannot affect G . The only effect is on the distance r , according to

$$r = r_0 + v \cdot \hat{r} t = F_0 + v_z t \quad (41)$$

The effect of (41) on the amplitude of the cylindrical wave is neglected, however, in the exponent we get the Doppler frequency shift described by (20). The transverse velocity component v_z has the same effect as in the case $v_z = 0$ discussed above, and the two effects are juxtaposed. We therefore obtain a spectrum as in Fig. 2(b), appropriately shifted according to v_z and with endpoints affected by v_z , as shown in Fig. 4. Corresponding to (31) we have for the present case

$$\delta(\nu - \omega) * \psi_a(k v_z \xi / F_0), \quad \omega_1 = \omega(1 - v_z / c) \quad (42)$$

and therefore, according to (22)

$$S(\nu) = \delta(\nu - \omega_1) * \psi_a(k v_z \xi / F_0) * \psi_a(k v_z \xi / F_0) \quad (43)$$

and if the pulse spectrum has a significant effect then (43) should be modified according to (28). The spectrum depicted in Fig. 4 describes a uniformly insinified aperture and provides a representative example.

The circular aperture transducer: The same argument used above for the long strip transducer applies here. The two effects of the v_x and v_z velocity components are compounded, hence by inspection of Figs. 3, 4 we conclude that for the present case the spectrum will be as in Fig. 5. Thus the spectrum is shifted due to v_z and the endpoints are determined by the maximum Doppler effect produced by the transducer's rim. For the present case (36) is modified by replacing $\delta(\nu - \omega)$ by $\delta(\nu - \omega_1)$, ω_1 as in (42) and changing v to v_x in the expression in braces (36). Similar modifications are performed in (37) which now contains $\delta(\nu - \omega_2)$ as in (22), leading to the appropriate form of (38) which yields the spectrum of Fig. 5.

TRANSVERSE MOTION, VELOCITY GRADIENTS

The long strip transducer: The geometry is the same as for constant velocity, however here the velocity $v(z)$ is in the x -direction and depends on z . For each particle the spectrum is as in Fig. 2. Due to the incoherent field produced by the

ensemble of particles, the combined spectrum is computed by adding intensities as in (30). The effect is the same as the peaking of the spectrum in Fig. 3, but the reasons are different. Obviously the largest velocity component produces the broadest spectrum, hence the endpoints of the spectrum profile correspond to the maximum velocity, as depicted in Fig. 6. The exact shape depends on the number of particles possessing various velocities and is too complicated for analytical computation. It is important to note that on integrating (8) the velocity may appear in the denominator, e.g., for $\psi = \text{const.}$ For the present case this means that a factor $\frac{1}{v(z)}$ appears in the expression $S(\nu, v)$, (30) for the spectrum of the single particle, and must be taken into account. In order to gain more insight, an idealized model is analysed in Appendix C.

The circular aperture transducer: This case is too complicated for analytical treatment. The best we can do is to make inferences from the other cases discussed above. Peaking of the spectrum is due to the special geometry, as explained above (see Fig. 3), even if the velocity is constant. On the other hand, from the discussion of the long strip transducer for velocity gradients (see Fig. 6), we expect similar peaking effects for the circular aperture transducer as well. We therefore have two mechanisms which affect the spectrum shape in the same way. Numerical calculations will be required to assess the relative significance of each mechanism. This is not done here. Anyhow, it is clear that the expected spectrum, sketched in Fig. 6, will be symmetrical with respect to $\nu = \omega$ and the endpoints will depend on the maximum velocity. To some extent the above conclusions are supported by the numerical simulations of Bascom et al.³, although they treat the case of a CW Doppler system.

OBLIQUE MOTION, VELOCITY GRADIENTS

The long strip transducer: Consider now oblique motion and velocity gradients, such that $v_x / v_z = \alpha$ remains constant, i.e., the velocity varies but its direction in space is constant. For a single particle the amplitude spectrum is given in Fig. 4 and the endpoint frequencies are $\nu = \omega \left[1 - v_z \left(\frac{2}{c} + \frac{W \alpha}{F_0 c} \right) \right]$.

The spectrum is symmetrical with respect to $\nu = \omega(1 - 2v_z / c)$. Now if v_z varies, the spectra corresponding to various particles having different velocities will be shifted on the ν axis, as well as become broader. Thus we have to add the corresponding power spectra as depicted in Fig. 7. The total amplitude spectrum is expected to have the shape shown in Fig. 8. If v_z is negative, i.e., the particles have a velocity component towards the transducer, then the expected spectrum will be as in Fig. 9. In Appendix D a semi-analytical discussion is given which supports the present conclusions.

The circular aperture transducer: The problem is too complicated for analytical discussion, hence a verbal argument is used once more. For a single velocity component the spectrum of Fig. 5 is expected, which qualitatively speaking is not different from Fig. 4 for the long strip transducer. Hence for the present case we expect spectra as in Figs. 8, 9, with W replaced by the diameter $2b_0$ of the circular transducer.

CONCLUDING REMARKS

Doppler spectra for various cases have been considered. The theory is based on the reciprocity principle and the Doppler spectra convolution theorem. The results are applied to long strip and circular aperture transducers, for cases of single velocity and velocity gradient fields. Both transverse and oblique motion is discussed. Conventional Doppler measurements are performed at oblique angles and the classical Doppler frequency shift is measured. The spectrum width is usually ignored in such measurements. This kind of measurement is not accurate for angles approaching the transverse direction. The spectrum becomes broader, and due to the statistical noise inherent in the system, the determination of the classical Doppler frequency becomes very inaccurate. On the other hand, by understanding the structure of the Doppler spectrum, information about the velocity can be derived from the spectrum, especially the endpoints, which turn out to be very quiet, consistent from one sampled spectrum to another. The present study is theoretical, but the results are in good agreement with previous analyses and experiments³⁻⁶. It should however be realized that the present discussion assumes perfect laminar flows, while in reality the noise produced by microturbulence cannot be neglected.

REFERENCES

1. T.P. Gill, *The Doppler Effect: An Introduction to the Theory of the effect*, Academic Press, 1965.
2. V.L. Newhouse, E.S. Furgason, G.f. Johnson and D.A. Wolf, "The dependence of ultrasound Doppler bandwidth on beam geometry", *IEEE Trans. on Sonics and Ultrasonics*, *SU-27*, 50-59, 1980.
3. P.A.J. Bascom, R.S.C. Cobbold and B.H.M. Roelofs, "Influence of spectral broadening on continuous wave Doppler ultrasound spectra: A geometric approach", *Ultrasound in Medicine and Biology*, *12*, 387-395, 1986.
4. J.A. Cisneros, "Medical applications of Doppler spectral analysis using a normal orientation of the beam with respect to the direction of flow", Ph.D. thesis submitted to the Faculty of Drexel University, 1985.
5. J.A. Cisneros, V.L. Newhouse and B. Goldberg, "Doppler spectral characterization of flow disturbances in the carotid with the Doppler probe at right angles to the vessel axis", *Ultrasound in Medicine and Biology*, *11*, 319-328, 1985.
6. J.A. Cisneros, B. Goldberg, D. Censor and V.L. Newhouse, "Ultrasound Doppler probing of flows transverse with respect to beam axis", submitted for publication; a portion of this paper was presented at the IEEE Ultrasound Conference, San Francisco, October 1985.
7. D.W. Baker, F.K. Foster and R.E. Daigle, "Doppler principles and techniques", in *Ultrasound: Its Application in Medicine and Biology*, ed. F.J. Fry, Vol. I, pp. 161-287, Elsevier, 1978.
8. V.L. Newhouse and I. Amir, "Time dilation and inversion properties and the output spectrum of pulsed Doppler flowmeters", *IEEE Trans. on Sonics and Ultrasonics* *SU-30*, 174-179, 1983.
9. P.M. Morse and K.U. Ingard, *Theoretical Acoustics*, McGraw-Hill, 1968.
10. J.D. Jackson, *Classical Electrodynamics*, Wiley, 1975.
11. M. Born and E. Wolf, *Principles of Optics*, Pergamon, 1980.
12. J.W. Goodman, *Introduction to Fourier Optics*, McGraw-Hill, 1968.

APPENDIX A: A SIMPLIFIED PROOF OF EQ. (2)

A detailed treatment is given elsewhere⁸, the present discussion is simplified, merely to show how (29) is obtained. The system transmits a train of pulses, at a repetition frequency Ω . A simple model representing such a signal is

$$h(t) = e^{-i\omega_0 t} \cos\Omega t \quad (A1)$$

i.e., a beat signal with carrier frequency ω_0 and repetition frequency Ω . Due to the Doppler effect, the echo at the receiver is

$$h_z(t) = e^{-i\omega_0 \beta t} \cos\Omega \beta t \quad (A2)$$

β being the Doppler factor appearing in (28). The mixing with ω_0 and subsequent filtering, which takes place in the receiver yields

$$e^{i\omega_0 \gamma t} \cos\Omega \beta t \quad (A3)$$

where $\gamma = 1 - \beta$ as in (29). The signal is then sampled by narrow pulses with the repetition frequency Ω . This provides a range gate such that the received echoes originate at a certain distance from the transducer. Because of the low pass filter following the sampler (or in some systems the sample and hold arrangement), only the lowest frequencies of the sampling signal are relevant to our discussion. Thus if (A3) is multiplied by $2\cos\Omega t$ and only the lowest frequencies are retained, we obtain

$$e^{-\omega_0 \gamma t'} \cos\Omega \gamma t' \quad , \quad t' = -t \quad (A4)$$

which is a compressed time inverted replica of (A1). The same relation as between (A1) and (A4) also exists between (27) and (29).

APPENDIX B: CIRCULAR APERTURE WITH GAUSSIAN APODIZATION; TRANSVERSE MOTION AND CONSTANT VELOCITY

The following analysis deals with a highly idealized model. The results support the conclusions derived above for the uniformly insonified aperture under the same circumstances.

Consider (33) for an aperture function

$$\psi_a(\rho) = \frac{1}{\sqrt{2\gamma}} e^{-\rho^2/(4\gamma)} \quad (B1)$$

where γ is a constant. The Gaussian apodization facilitates analysis for certain limiting cases. For the long strip transducer (31), a Gaussian aperture would lead to a Gaussian spectrum. For the circular aperture we have (33), and for small γ (B1) falls off rapidly, hence we are justified in approximating

$$J_0(k\rho\sin\theta) \approx 1 - \left(\frac{k\rho\sin\theta}{2}\right)^2 \approx e^{-\frac{(k\rho\sin\theta)^2}{2}} \quad (B2)$$

Hence (33) becomes

$$\begin{aligned} \frac{2\pi}{\sqrt{2\gamma}} \int_0^\infty \rho d\rho e^{-\rho'^2} &= \frac{4\pi}{\sqrt{2\gamma}} \frac{1}{1/\gamma + k^2 \sin^2\theta} \int_0^\infty d(\rho'^2) e^{-\rho'^2} \\ \frac{4\pi}{\sqrt{2\gamma}} \frac{1}{\gamma + k^2 \sin^2\theta} &= \frac{d}{a^2 + t^2} \quad , \quad \rho'^2 = \rho^2(1/\gamma + k^2 \sin^2\theta)/4 \\ d &= \frac{4\pi}{\sqrt{2\gamma}} \frac{F_0^2}{k^2 v^2} \quad , \quad a = \frac{F_0}{kv} \left(\frac{1}{r} + \frac{k^2 y^2}{F^2} \right) \end{aligned} \quad (B3)$$

and $\sin\theta$ is given in (34), and we put $r_0 = F_0$, the focal length.

From a table of Fourier transforms one finds that the spectrum of $\frac{d}{a^2 + t^2}$ is given by $\frac{\sqrt{\pi}}{2} \frac{d}{a} e^{-a|\nu|}$. It follows that for large y , i.e., larger a , the amplitude at $\nu = 0$ is smaller and $e^{-a|\nu|}$ falls off faster, i.e., the spectrum is narrower. This result agrees with the sketch in Fig. 3(a) and therefore supports the ensuing spectrum in Fig. 3(b).

APPENDIX C: LONG STRIP TRANSDUCER WITH GAUSSIAN APODIZATION; TRANSVERSE MOTION AND VELOCITY GRADIENTS

Let the aperture function have the Gaussian form

$$\psi_a(\xi) = \frac{1}{\sqrt{2\beta}} e^{-\xi^2/(4\beta)} \quad (C1)$$

where β is a constant. For a single particle (8), (9) prescribe

$$\int e^{-i\nu t} G(\nu) dt = K \frac{F_0 c}{\omega v} \int e^{-i\nu \xi} \psi(\xi) d\nu_\xi, \quad \nu_\xi = \frac{\omega v \xi}{c F_0} \quad (C2)$$

where K is a proportionality factor. Therefore

$$G(\nu) = K \frac{F_0 c}{\omega v} \frac{1}{\sqrt{2\beta}} e^{-\left(\frac{F_0 \nu c}{\omega v 2\sqrt{\beta}}\right)^2} = K \frac{1}{\sqrt{2\beta}} e^{-\nu^2/4\beta} \quad (C3)$$

$$\beta = \beta \left(\frac{\omega v}{F_0 c}\right)^2$$

We find $S(\nu, v)$ from (18), but instead of convolving (C3), we

use the transform $G(\mu) = F\left\{G(\nu)\right\} = K e^{-\beta^* \mu^2}$. Squaring yields

$$[G(\nu)]^2 = K^2 e^{-2\beta^* \mu^2} = K^2 e^{-\beta^* \mu^2}, \quad \beta^* = 2\beta \quad (C4)$$

Hence

$$G(\nu) * G(\nu) = K^2 \frac{1}{\sqrt{2\beta^*}} e^{-\nu^2/4\beta^*} = \frac{K^2 F_0 c}{2\sqrt{\beta} \omega v} e^{-\frac{\nu^2}{8\beta} \left(\frac{F_0 c}{\omega v}\right)^2} \quad (C5)$$

is Gaussian once more. In order to compute (30) $f(v)$ must be chosen in $S(\nu)$

$$S(\nu) = \left\{ \frac{K^2 F_0 c}{2\omega\sqrt{\beta}} \int_{v_1}^{v_2} dv \frac{e^{-A/\nu^2}}{v^2} f(v) \right\}^{1/2},$$

$$A = \frac{1}{\beta} \left[\frac{(\nu-\omega) F_0 c}{2\omega} \right]^2 \quad (C6)$$

Noting that $\frac{d}{dv} e^{-A/\nu^2} = \frac{2A}{v^3} e^{-A/\nu^2}$, we choose $f(v) = \frac{1}{v}$. Hence (C6) becomes

$$S(\nu) = \left\{ \frac{K^2 F_0 c}{4\sqrt{\beta}\omega A} \int_{v_1}^{v_2} dv \frac{d}{dv} e^{-A/\nu^2} \right\}^{1/2}$$

$$= \left\{ \frac{K^2 F_0 c}{4\sqrt{\beta}\omega A} (e^{-A/\nu_2^2} - e^{-A/\nu_1^2}) \right\}^{1/2} \quad (C7)$$

In order to check the limit $A \rightarrow 0$, to ensure that $S(\nu)$ does not become singular, we expand the exponentials near the origin. This yields

$$\lim_{A \rightarrow 0} S(\nu) = \frac{K^2 F_0 c}{4\sqrt{\beta}\omega} \left(\frac{1}{\nu_1^2} - \frac{1}{\nu_2^2} \right) \quad (C8)$$

The results of this analysis support the semi-quantitative argument leading to Fig. 6. Near $\nu = \omega$, i.e., near $A = 0$, $S(\nu)$ (C7) is dominated by the factor $\frac{1}{A}$ which produces peaking in the spectrum. Since $V_2 > V_1$, e^{-A/ν_2^2} falls off slowly compared to e^{-A/ν_1^2} , therefore for large A , i.e., $\nu \gg \omega$ the shape is dominated by the maximum velocity, as anticipated in Fig.6. Also note that $S(\nu)$, (C7) is symmetrical with respect to $\nu = \omega$, as expected.

APPENDIX D: LONG STRIP TRANSDUCER WITH GAUSSIAN APODIZATION; OBLIQUE MOTION AND VELOCITY GRADIENTS

For the present case (C3), (C5) are modified by changing

v to $v_z = \alpha_z$ and in (C6) $\nu - \omega$ is changed to $\nu - \omega(1-2v_z/c)$. Thus we now have

$$S(\nu) = \left\{ \frac{K^2 F_0 c}{2\sqrt{\beta}\omega\alpha} \int_{v_{z1}}^{v_{z2}} \frac{dv_z}{v_z^2} e^{-A/(\alpha v_z)^2} f(\alpha v_z) \right\}^{1/2}$$

$$A = \frac{1}{\beta} \left[\frac{\nu - \omega(1-2v_z/c)}{2\omega} F_0 c \right]^2 \quad (D1)$$

By changing the variable we obtain

$$S(\nu) = \left\{ \frac{K'}{1 - \frac{\nu}{\omega}} \int_{u_1}^{u_2} du e^{-u^2} f(\alpha v_z) \right\}^{1/2}$$

$$u^2 = \left[\frac{F_0 c}{2\sqrt{\beta}\alpha} \left(\frac{\nu/\omega - 1}{v_z} + \frac{2}{c} \right) \right]^2$$

$$du = \pm \frac{F_0 c}{2\sqrt{\beta}} \frac{\nu/\omega - 1}{\alpha v_z^2} dv_z \quad (D2)$$

where K' is a constant and the sign of du is chosen such that $S(\nu)$ is real (i.e., the expression in braces in (D1) is positive). By choosing $f(\alpha v_z) = 0$ and writing $\int_{u_1}^{u_2} = \int_0^{u_2} - \int_0^{u_1}$, (D2) is representable in terms of the error function. Thus we have

$$S(\nu) = \left\{ \frac{K'}{1 - \frac{\nu}{\omega}} [\text{erf}(u_2) - \text{erf}(u_1)] \right\}^{1/2}$$

$$u_1 = F_0 \frac{c}{2\sqrt{\beta}\alpha} \left(\frac{\nu/\omega - 1}{v_{z1}} + \frac{2}{c} \right) \quad (D3)$$

and a similar expression for with v_{z2} for u_2 . It follows that (D3) describes the square root of the difference of two displaced error functions, further multiplied by $(1-\nu/\omega)^{-1}$, as sketched in Fig. 10. By inspection of Fig. 10 it becomes clear that (D3) is consistent with the amplitude spectrum shape derived in Fig. 8.

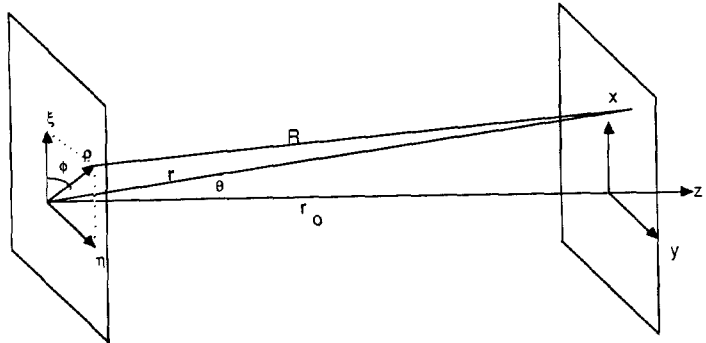
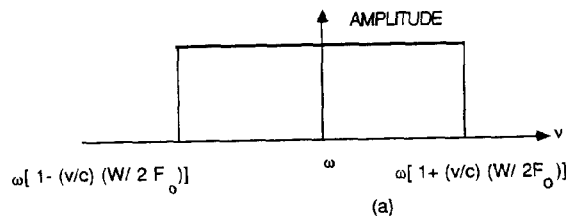


Fig. 1: Source-observer geometry



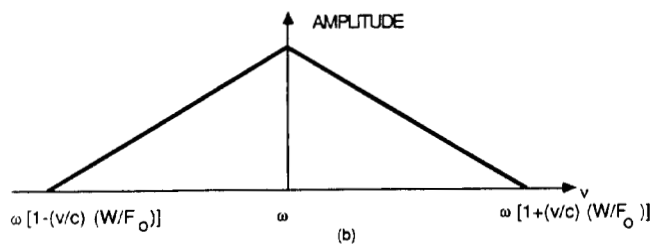


Fig. 2: Long strip transducer with uniformly insonified aperture. (a) amplitude spectrum of the field exciting the particle; (b) amplitude spectrum for the echo signal.

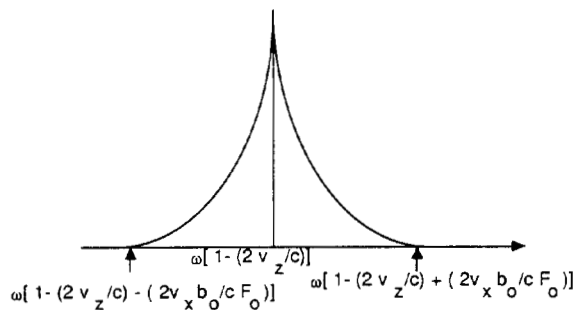


Fig. 5: Amplitude spectrum for circular aperture transducer for constant velocity and oblique incidence.

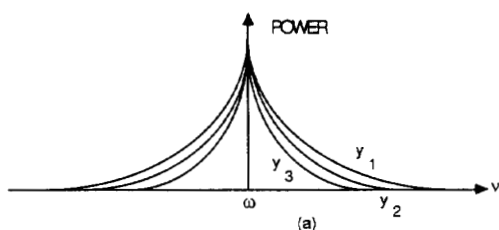


Fig. 3: (a) sketches for power spectra for $y_1 < y_2 < y_3$ for circular aperture; (b) sketch of the peaked amplitude spectrum due to the combined effect of particles traversing the focal plane at various off axis distances.

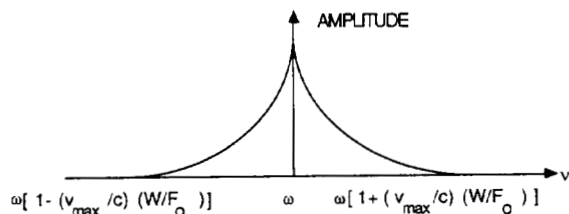


Fig. 6: Amplitude spectrum for long strip transducer for transverse motion and velocity gradients.

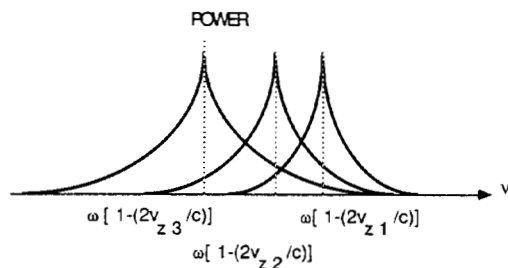
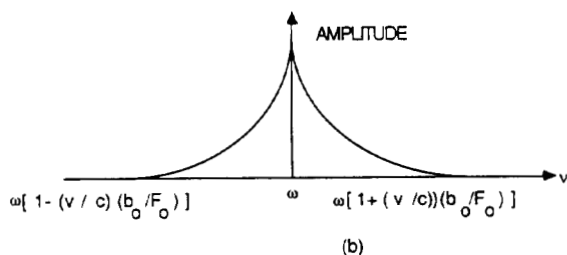


Fig. 7: Addition of power spectra for long strip transducer, oblique motion and velocity gradients.

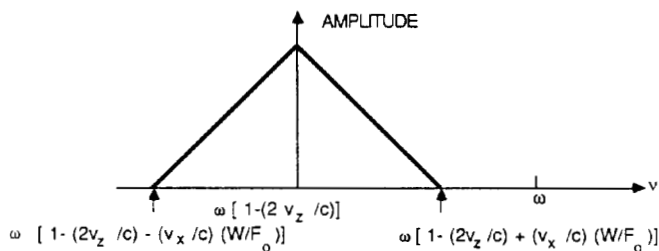


Fig. 4: Amplitude spectrum for long strip transducer for constant velocity and oblique incidence.

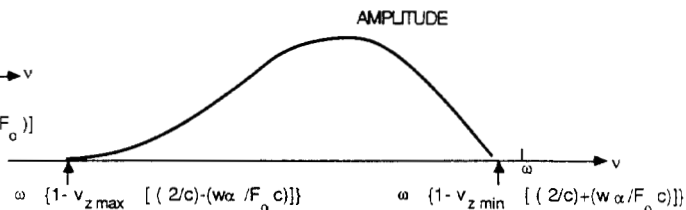


Fig. 8: Amplitude spectrum for long strip transducer, oblique motion and velocity gradients for the case $v_z > 0$.

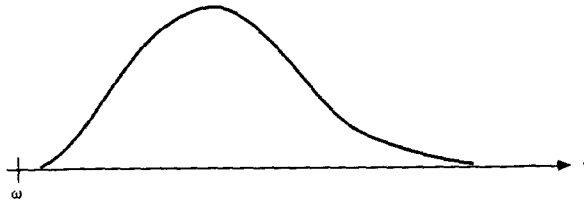


Fig. 9: As in Fig. 8, but $v_2 < 0$.

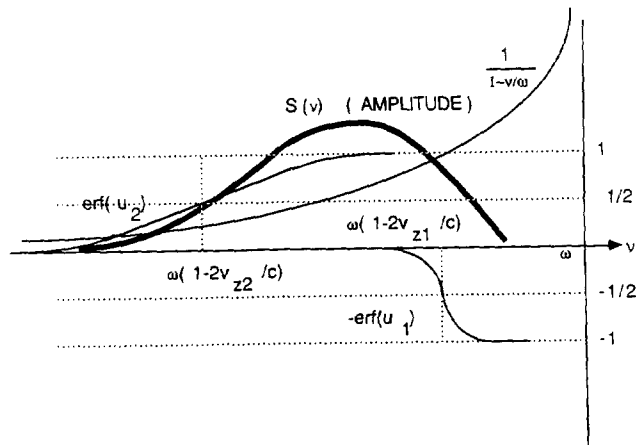


Fig. 10: Relevant to the analysis for oblique incidence and velocity gradients, Appendix C. The result is consistent with the shape obtained in Fig. 8.